Development of Synchrophasors Measuring Method for Power Systems

K. Seki

***Abstract*—This paper proposes synchrophasors measuring method for power systems. At first, a new frequency measuring method by using spiral vector is introduced. Then the phasor is defined in the upper half-plane and measured by using least square method. Then time and space synchrophasors are defined and measured by using the uncertainty principles of synchrophasors. The numerical simulation result shows that the proposed method is practical. At last, the paper analyzes accuracy, step test and harmonic distortion influence of the proposed method.**

***Keywords*: phasor, time synchrophasor, space synchrophasor, frequency measurement, least square method.**

I. INTRODUCTION

PMUs (phasor measurement units) are becoming more and more important for power systems today. Because conventional methods measure synchrophasors first and use an analog reference wave, they demand to the discrete Fourier transform (DFT) or positive sequence component transform to estimate synchrophasors [1]. On the other hand, spiral vector theory is a new AC circuits and machines theory and its state variables are expressed as spiral vectors that rotating counterclockwise in the complex plane [2]. We have developed a new frequency measuring method by using spiral vectors [5]. We also have developed a new synchrophasors measuring method by using an inverse cosine function. In this paper, we improve and expand definitions for time and space synchrophasors and introduce the uncertainty principles of synchrophasors. The new method uses single-phase data and it only demands a coordinated universal time (GPS) for measuring space synchrophasor. The difference between the proposed method and conventional methods are the former demands neither DFT transformation nor an analog reference wave and the latter need both of them.

The following parts of the paper is organized as follows: section II introduces frequency measuring method, section III introduces the phasor measuring method by using least square method, section IV proposes time and space synchrophasors measuring method by using the uncertainty principles, section V analyzes accuracy, step test and harmonic distortion influence of the new method, and section VI is the conclusion.

K.Seki is with Protection & Control Systems Department, Mitsubishi Electric Corporation, Kobe 651-2271 Japan (e-mail of corresponding author: Seki.Kempei@dc.MitsubishiElectric.co.jp).

Paper submitted to the International Conference on Power Systems Transients (IPST2009) in Kyoto, Japan June 3-6, 2009

II. MEASURING FREQUENCY BY USING SPIRAL VECTORS

This section introduces a new frequency measuring method for power systems [5].

A. The novel idea of frequency measurement

According to the novel idea shown in Fig. 1, the frequency can be calculated as follows

$$f_1(t) = \frac{\psi(t)}{2\pi} f_0 \tag{1}$$

where f_0 is the one of two nominal frequencies 50Hz or 60 Hz exist in power systems. The rotation phase angle $\psi(t)$ can be calculated as follows

$$\psi(t) = \frac{1}{T_0}\int_{-T_0}^{0} d\psi(t)dt \tag{2}$$

where T_0 is one period time of the nominal frequency as follows

$$T_0 = \frac{1}{f_0} \tag{3}$$

According to (1), if the rotation phase angle $\psi(t)$ is 2π, actual frequency equals to the nominal power system frequency. This novel idea changes the problem of frequency measurement from how to find a zero crossing point of a sine wave to calculate the rotation phase angle in the complex plane. Because the new method is an integral calculation method and the conventional method is a differential calculation method, it is understood that the former is stable and the latter is unstable generally.

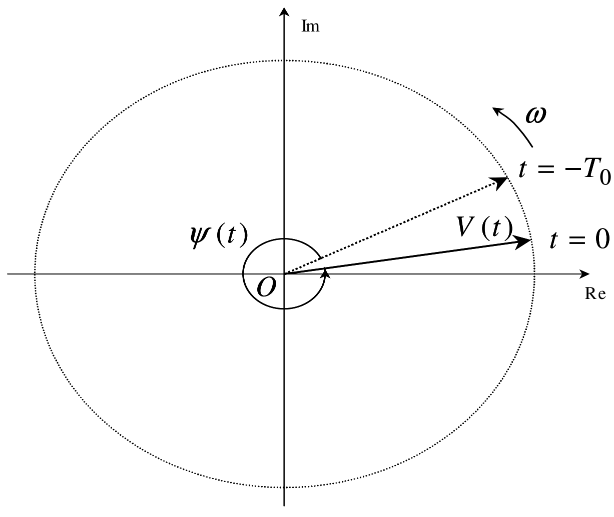

Fig. 1. A voltage spiral vector in the complex plane

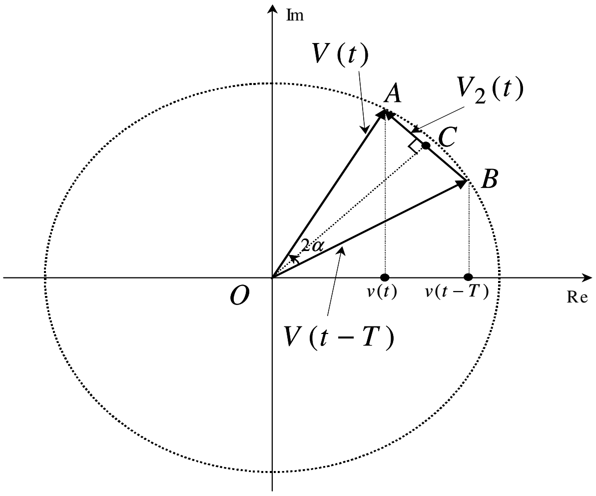

Fig. 2. A voltage spiral vector is rotating in one pitch period in the complex plane.

B. Measuring amplitude and chord length of a spiral vector voltage with common integral equations

The voltage of single-phase in power systems can be expressed as

$$v_c(t) = Ve^{j(\omega t+\varphi)} + \sum_{h=1}^{M} V_h e^{j(\omega_h t+\varphi_h)} \tag{4}$$

where the first term is the fundamental frequency component and the second term is harmonics distortions. All terms are spiral vectors. The voltage instantaneous values are the real part of the spiral vectors as

$$v(t) = V\cos(\omega t+\varphi) + \sum_{h=1}^{M} V_h \cos(\omega_h t+\varphi_h) \tag{5}$$

We will use the fundamental frequency component when introducing new method. The second term of right side of (5) has little influence to the measured results because the proposed method using integration processing can negate harmonics component. The details is explained in section V.

A voltage spiral vector rotating in one pitch period in the complex plane is shown in Fig.2. The amplitude of the spiral vector that is the length of OA in Fig.2 can be mathematically determined as

$$V(t) = \sqrt{\frac{2}{T_0}\int_{-T_0}^{0} v^2(t)dt} \tag{6}$$

where T_0 is one period time as expressed in (3). If assuming sampling frequency is

$$f_S = 4N f_0 \tag{7}$$

where N is a positive integer, we can obtain T that is one pitch period as

$$T = \frac{T_0}{4N} = \frac{1}{4N f_0} \tag{8}$$

TABLE I
PARAMETERS USED FOR CASE1 SIMULATION

Sampling Frequency	Input Frequency	Amplitude
600Hz	50Hz	45V

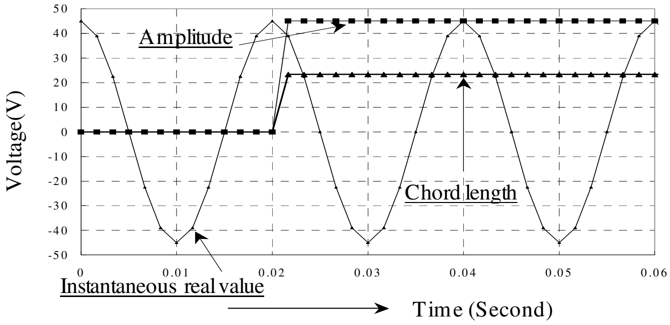

Fig. 3. Voltage instantaneous real values, measured amplitude and chord length with proposed integral method (Case1).

If the pitch of the calculation is set to T expressed as (8), the amplitude can be obtained as

$$V(t) = \sqrt{\frac{1}{2N}\sum_{k=0}^{4N-1} v^2(t-kT)} \tag{9}$$

The chord length of the spiral vector voltage that is the length of AB in Fig.2 can be mathematically determined as

$$V_2(t) = \sqrt{\frac{2}{T_0}\int_{-T_0}^{0} \{v(t)-v(t-T)\}^2 dt} \tag{10}$$

Same as (9), the chord length can be calculated as follows

$$V_2(t) = \sqrt{\frac{1}{2N}\sum_{k=0}^{4N-1} [v(t-kT) - v\{t-(1+k)T\}]^2} \tag{11}$$

Here a numerical simulation Case1 is executed. The parameters of Table I is used and the simulation result is shown in Fig.3. The chord length can be calculated theoretically by the following equation from the Pythagorean theorem. (In this case, the rotation phase angle is $\pi/6$ radian with respect to one sampling timing rotation phase angle).

$$V_2 = 2V\cdot\sin\frac{\pi}{12} = 23.2937(V) \tag{12}$$

The result of above (12) and input amplitude completely agrees with Fig.3 respectively and it is understood that proposed integral method is correct. We call (9) and (11) as common integral equations. But if input frequency shifts from the nominal frequency, the measured amplitude and chord length will be vibrated and the solution is not stable. With the help of mathematical theory, we overcome this difficult. The detailed equations will be shown next.

C. Measuring amplitude and chord length of a spiral vector voltage with difference integral equations

We propose a novel equation to calculate amplitude of a spiral vector as follows

$$V(t) = \sqrt{\frac{1}{2N}\left[\sum_{k=N}^{3N-1} v^2(t-kT) - \sum_{k=0}^{2N-1} v(t-kT)\cdot v\{t-(2N+k)T\}\right]} \tag{13}$$

The above equation can negate vibration of amplitude by using the difference in spiral vectors in one period time. We call it as difference integral equation.

TABLE II
PARAMETERS USED FOR CASE2 SIMULATION

Sampling Frequency	Input Frequency	Amplitude
600Hz	45Hz	45V

Assuming the nominal frequency is 50Hz and the sampling frequency is 600Hz, (13) becomes

$$V(t)=\sqrt{\frac{1}{6}\left[\sum_{k=3}^{8}v^2(t-kT)-\sum_{k=0}^{5}v(t-kT)\cdot v\{t-(6+k)T\}\right]} \quad (14)$$

The amplitude measured simulation with parameters that are listed in Table II is executed and the result is shown in Fig.4. It is illustrated that the measured amplitude of common integral equation is greatly vibrated, but the result of difference integral equation is stable.

In the same way, we propose difference integral equation to calculate the chord length of a spiral vector as follows

$$V_2(t)=\sqrt{\frac{1}{2N}\left[\sum_{k=N}^{3N-1}{v_2}^2(t-kT)-\sum_{k=0}^{2N-1}v_2(t-kT)\cdot v_2\{t-(2N+k)T\}\right]} \quad (15)$$

Assuming the nominal frequency is 50Hz and the sampling frequency is 600Hz, (15) becomes

$$V_2(t)=\sqrt{\frac{1}{6}\left[\sum_{k=3}^{8}{v_2}^2(t-kT)-\sum_{k=0}^{5}v_2(t-kT)\cdot v_2\{t-(6+k)T\}\right]} \quad (16)$$

The chord length measured simulation with parameters of Table II is executed and the result is shown in Fig. 5. It is illustrated that the measured chord length of common integral equation is greatly vibrated, but the result of difference integral equation is stable.

Accordingly, difference integral equations negate vibration arising from actual frequency shifts the nominal frequency.

D. Measuring the rotation phase angle and frequency by using the Pythagorean theorem

Refer to Fig.2, if assuming that two amplitudes equal to each other, the following equation is realized for this isosceles triangle

$$\alpha=\angle AOC=\angle BOC \quad (17)$$

where the rotation phase angle 2α is the central angle at one sampling pitch from a certain timing to the next timing. According to the Pythagorean theorem, the half central angle can be calculated as follows

$$\alpha(t)=\sin^{-1}\frac{V_2(t)}{2V(t)} \quad (18)$$

where *V(t)* is the measured amplitude and $V_2(t)$ is the measured chord length. So the rotation phase angle in one period time can be obtained as

$$\psi(t)=8N\cdot\alpha(t) \quad (19)$$

Substituting (19) into (1), actual frequency can be obtain as

$$f_1(t)=\frac{4N\cdot\alpha(t)}{\pi}f_0 \quad (20)$$

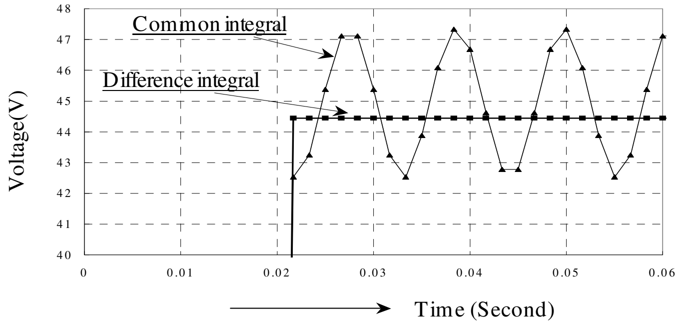

Fig. 4. Measured amplitudes with common integral method and difference integral method (Case2).

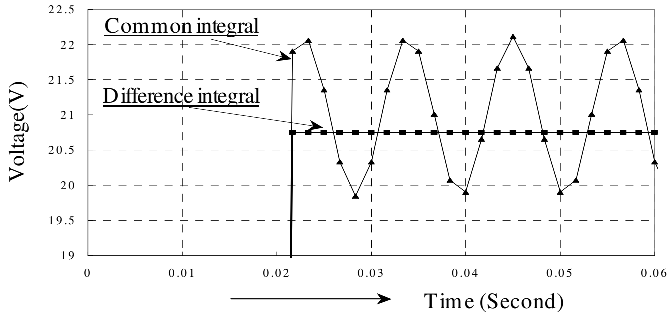

Fig. 5. Measured chord lengths with common integral method and difference integral method (Case2).

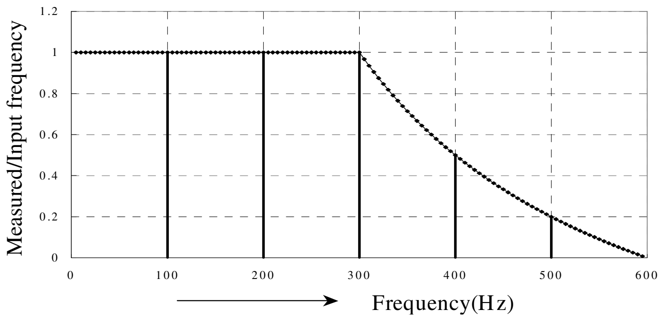

Fig. 6. Gain characteristics curve with the proposed method (Case3).

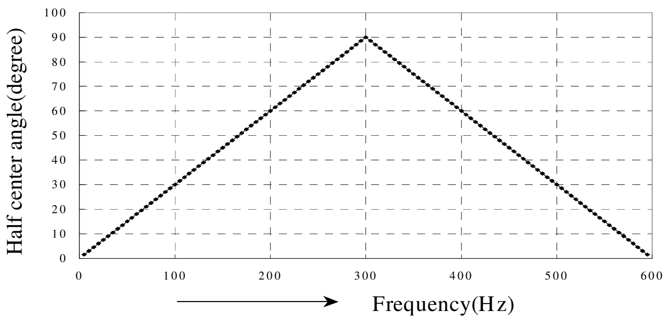

Fig. 7. Measured half central angle at a time step curve with the proposed method (Case3).

TABLE III
PARAMETERS USED FOR CASE3 SIMULATION

Sampling Frequency	Input Frequency	Amplitude
600Hz	5-600Hz	45V

The Case3 simulation with parameters of Table III is executed and the results are shown in Fig.6-8. Figure 6 shows gain characteristics between ratio of precision and input frequency with the proposed integral method. It shows that there are several singular points (100/200/300/400/500Hz) because the measured amplitude and chord length both become zero at these points that are shown in Fig. 8.

Figure 7 shows the half central angle of a time step with the proposed integral method.

Figure 8 shows the measured amplitude and chord length of the spiral vector voltage. The following remarks should be made. The measured amplitude and chord length are different with real amplitude and chord length of input wave.

Figure 9 shows comparison of the common integral method and the difference integral method with parameters of Table II, it is illustrated that the former is greatly vibrated and the latter is stable.

The above results agree with famous Nyquist–Shannon sampling theorem that the upper bound for frequency measurement is the half of the sampling frequency.

III. Measuring The Phasor By Using Least Square Method

This section defines the phasor and measures it with least square method [6].

A. Defining the phasor in the upper half-plane

We define the phasor as an inverse cosine function as in [6].

$$\alpha(t) = \cos^{-1}\left\{\frac{v(t)}{V(t)}\right\} \tag{21}$$

where $v(t)$ is the instantaneous real value of the spiral vector voltage and V(t) is the amplitude of the spiral vector voltage shown in Fig.10.

Here simulation by using parameters of Case1 is executed for the phasor measurement. The simulation result is shown in Fig. 11. According to the new definition, the phasor changes between $0 \sim \pi$ in the upper half-plane, and always possesses a positive value.

If actual frequency shifts the nominal frequency, the result of (21) will also shift the real phasor that is on the actual frequency. We introduce least square method to obtain the real phasor with the measured frequency next.

B. Measuring the phasor with least square method

The instantaneous real value of the spiral vector voltage expressed in (5) can transform to (only fundamental frequency component is used)

$$v(t) = V\cos(\omega t + \varphi) = P_1 \cos\omega t + P_2 \sin\omega t \tag{22}$$

where P_1 and P_2 are arbitrary constants and can obtained by using least square method as follows

$$[P] = ([A]^T[A])^{-1}[A]^T[v] \tag{23}$$

The arbitrary coefficient matrix is

$$[P] = \begin{bmatrix} P_1 \\ P_2 \end{bmatrix} \tag{24}$$

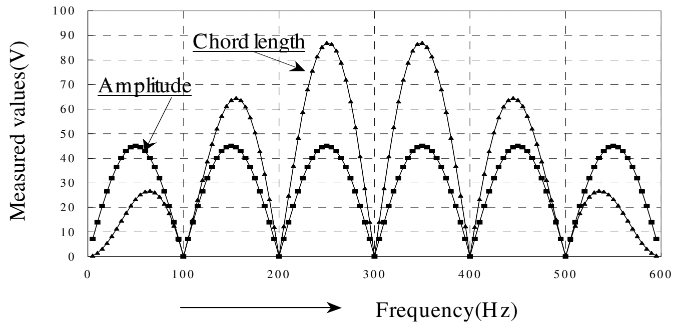

Fig. 8. Measured amplitude and chord length curves with the proposed method (Case3).

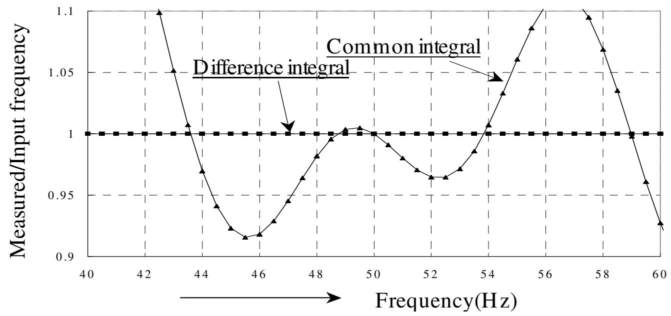

Fig. 9. Measured gain characteristics curves with common integral and difference integral method (Case2).

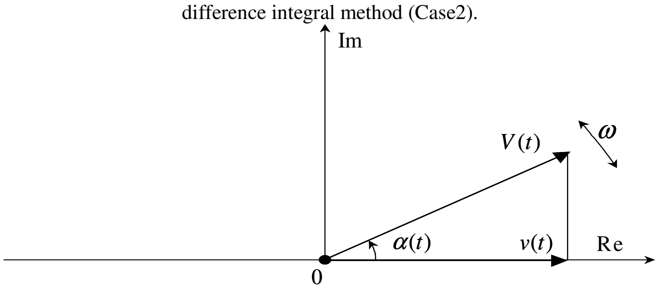

Fig. 10. Defining the phaor in the complex plane.

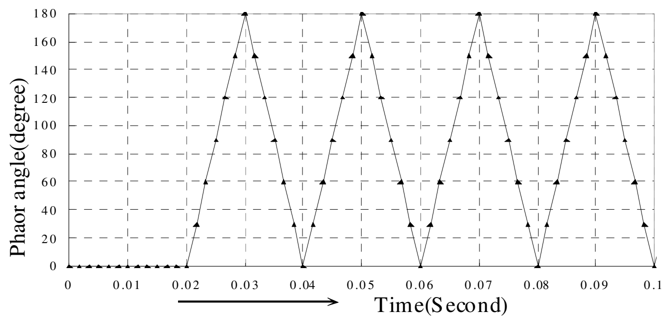

Fig. 11. Measured phasor with the proposed method (Case1).

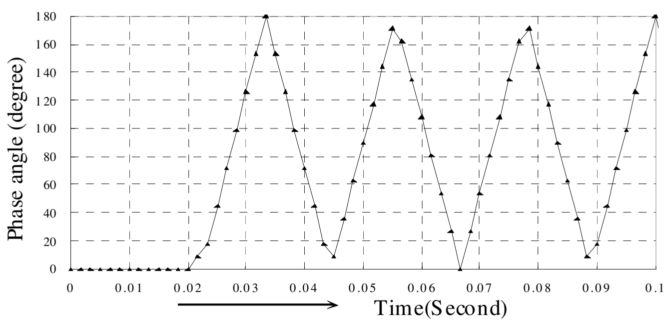

Fig. 12. Measured phasor with the proposed method (Case2).

The voltage instantaneous real value matrix is

$$[v]=\begin{bmatrix} v_1 \\ v_2 \\ \vdots \\ v_{4N} \end{bmatrix} \tag{25}$$

The trigonometric matrix is

$$[A]=\begin{bmatrix} \cos\omega_1 t_1 & \sin\omega_1 t_1 \\ \cos\omega_1 t_2 & \sin\omega_1 t_2 \\ \vdots & \vdots \\ \cos\omega_1 t_{4N} & \sin\omega_1 t_{4N} \end{bmatrix} \tag{26}$$

where the radian frequency ω_1 is

$$\omega_1 = 2\pi f_1 \tag{27}$$

where f_1 is the measured frequency.

The series of time data is expressed as follows

$$\left.\begin{aligned} t_1 &= 0 \\ t_2 &= T \\ &\vdots \\ t_{4N} &= (4N-1)T \end{aligned}\right\} \tag{28}$$

where T is one pitch period expressed in (8).

The voltage estimated instantaneous real value is obtained as follows

$$v_{est}(t) = P_1 \cos\omega_1 t_{4N} + P_2 \sin\omega_1 t_{4N} \tag{29}$$

The voltage estimated amplitude is obtained as follows

$$V_{est}(t) = \sqrt{\frac{1}{2N}\sum_{k=0}^{4N-1} v^2{}_{est}\{t - kT_1(t)\}} \tag{30}$$

where the pitch period $T_1(t)$ should calculate from the measured frequency as follows

$$T_1(t) = \frac{1}{4N\ f_1(t)} \tag{31}$$

We obtain the real phasor as follows

$$\alpha(t) = \cos^{-1}\left\{\frac{v_{est}(t)}{V_{est}(t)}\right\} \tag{32}$$

A numerical simulation using parameters of Table II is shown in Fig.12.

C. Defining the mode of phasor rotation

For measuring synchrophasors, we define the mode of phasor rotation as follows

$$\alpha_m(t) = \begin{cases} 1; & [\alpha(t) > \alpha(t-T) > \alpha(t-2T)] \\ -1; & [\alpha(t) < \alpha(t-T) < \alpha(t-2T)] \\ 0; & [others]. \end{cases} \tag{33}$$

Three modes of above (33) will be explained as follows.

Mode1: The rotation phase angle of the phasor is becoming larger and larger as shown in Fig. 13, it is defined as the forward mode and its value is equal to 1.

Mode2: The rotation phase angle of the phasor is becoming smaller and smaller as shown in Fig. 14, it is defined as the backward mode and its value is equal to -1.

Mode3: If the phasor is neither a forward phasor nor a backward phasor, it is defined as the inversion mode and its value is 0. One inversion phasor is shown in Fig.15.

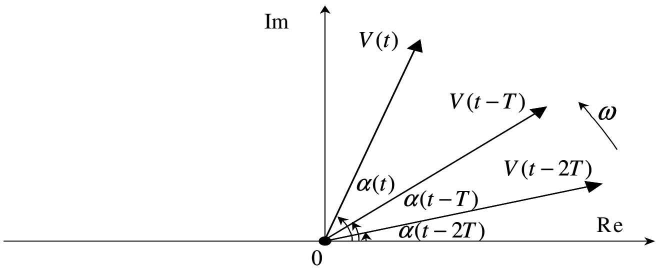

Fig. 13. A phasor is rotating in a forward mode.

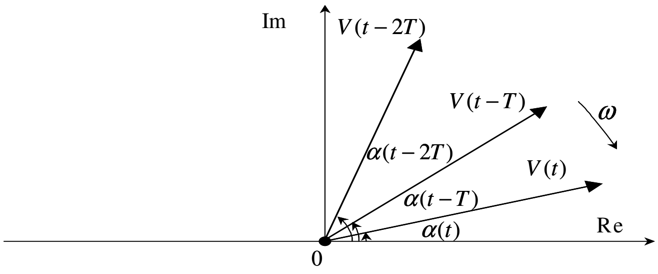

Fig. 14. A phasor is rotating in a backward mode.

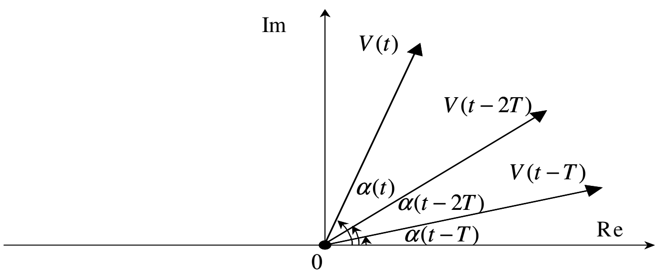

Fig. 15. A phasor is rotating in an inversion mode.

IV. MEASURING SYNCHROPHASORS

In this section, we propose measuring method for space and time synchrophasors.

A. Measuring space synchrophasor

The model system for measuring space synchrophasors is shown in Fig. 16 next page. We define space synchrophasor as space interval of two phasors that are node1 and node2 as follows ($\alpha_1(t)$ is preceding $\alpha_2(t)$)

$$\alpha_{SP}(t) = \begin{cases} \alpha_1(t) - \alpha_2(t); & [\alpha_{1m} = 1, \alpha_{2m} = 1] \\ \alpha_2(t) - \alpha_1(t); & [\alpha_{1m} = 1, \alpha_{2m} = -1] \\ \alpha_1(t) + \alpha_2(t); & [\alpha_{1m} = -1, \alpha_{2m} = -1] \\ 2\pi - \alpha_1(t) - \alpha_2(t); & [\alpha_{1m} = -1, \alpha_{2m} = 1] \\ \alpha_{SP}(t-T); & [\alpha_{1m} = 0\ or\ \alpha_{2m} = 0]. \end{cases} \tag{34}$$

where $\alpha_1(t)$ is the phasor of node1, $\alpha_2(t)$ is the phasor of node2, α_{1m} is the mode of node1 and α_{2m} is the mode of node2 respectively. It can be found that same as the phasor, space synchrophasor changes between $0 \sim \pi$ in the upper half-plane, and always possesses a positive value.

Because space synchrophasor measures two different place phasor, it demands universal precise time reference (GPS) to synchronize two phasors.

Five rows of above (34) will be explained as follows.

Row1: The phasor of node1 and the phasor of node2 both are in forward mode, space synchrophasor is in a forward-forward mode. One example of this mode is shown in Fig.17.

Row2: The phasor of node1 and the phasor of node2 both are in backward mode, space synchrophasor is in a backward-backward mode. One example of this mode is shown in Fig.18.

Row3: The phasor of node1 is in a forward mode and the phasor of node2 is in a backward mode, space synchrophasor is in a forward-backward mode. One example of this mode is shown in Fig.19.

Row4: The phasor of node1 is in a backward mode and the phasor of node2 is in a forward mode, space synchrophasor is in a backward -forward mode. One example of this mode is shown in Fig.20.

Row5: The phasor of node1 is in an inversion mode or the phasor of node2 is in an inversion, space synchrophasor is in a latch mode. One example of this mode is shown in Fig.21. We call it as the uncertainty principle of space synchrophasors because of this mode exists.

Fig. 16. The model system used for measuring space synchrophasor.

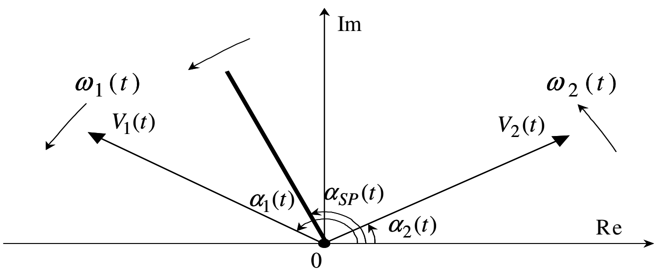

Fig. 17. A space synchrophasor is changing in a forward-forward mode.

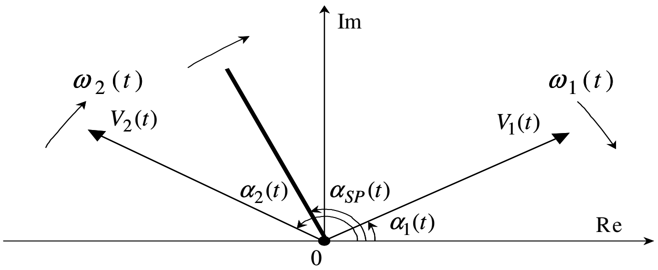

Fig.18. A space synchrophasor is changing in a backward-backward mode.

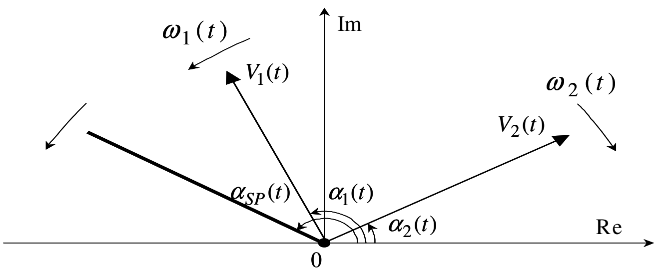

Fig. 19. A space synchrophasor is changing in a forward-backward mode.

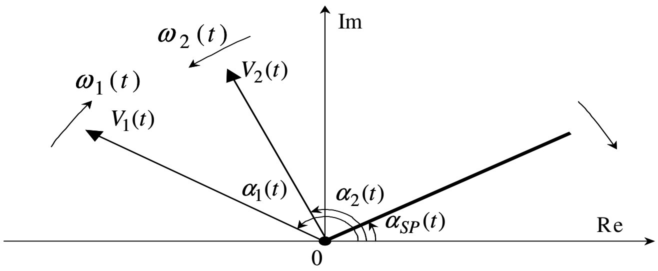

Fig. 20. A space synchrophasor is changing in a backward-forward mode.

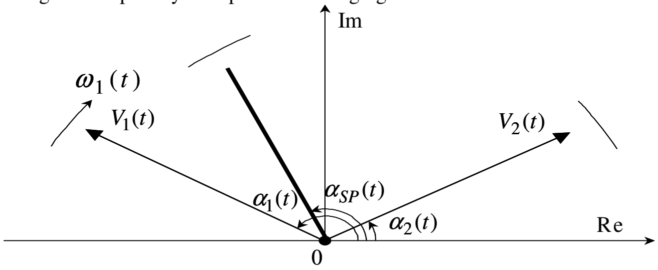

Fig. 21. A space synchrophasor is changing in a latch mode.

B. Measuring time synchrophasor

We define time synchrophasor as time interval of two phasors as follows (*$\alpha_1(t)$* is preceding *$\alpha_2(t)$*)

$$\alpha_{TP}(t)=\begin{cases}\alpha_1(t)-\alpha_2(t); & [\alpha_{1m}=1,\alpha_{2m}=1]\\ \alpha_2(t)-\alpha_1(t); & [\alpha_{1m}=1,\alpha_{2m}=-1]\\ \alpha_1(t)+\alpha_2(t); & [\alpha_{1m}=-1,\alpha_{2m}=-1]\\ 2\pi-\alpha_1(t)-\alpha_2(t); & [\alpha_{1m}=-1,\alpha_{2m}=1]\\ \alpha_{SP}(t-T); & [\alpha_{1m}=0\ or\ \alpha_{2m}=0]\end{cases} \tag{35}$$

where *$\alpha_1(t)$* is the phasor of now and *$\alpha_2(t)$* is the phasor of one or several period time ago as follows

$$\alpha_2(t)=\alpha_1(t-nT_0) \tag{36}$$

where *n* is a positive integer and *T_0* is one period time of the nominal frequency. Same as space synchrophasor, five modes of time synchrophasor can be referred in Fig. 17-21 and it also possesses a positive value in the upper half-plane.

C. Outlining synchrophasors measuring method

The procedure for measuring synchrophasors is shown in Fig. 22. Step6/7 is for measuring space synchrophasor that demands a GPS system and communication system devices.

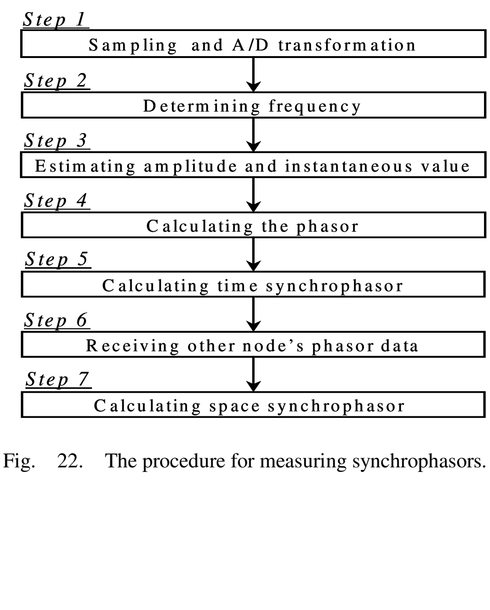

Fig. 22. The procedure for measuring synchrophasors.

D. Numerical Simulation Examples

Here we will execute several numerical examples to show the effective of the proposed method. The nominal frequency is 50Hz and the sampling frequency of these cases is 600Hz.

Figure 23 shows the measured phasor and time synchrophasor simulation with parameters of Table II. Because the time interval is set to two period times, time synchrophasor can be theoretically calculated as

$$\alpha_{TP} = \frac{f_0 - f_1}{f_0} 4\pi = \frac{50-45}{50} 4\pi = \frac{2\pi}{5} (radian) \tag{37}$$

The above result agrees with the simulation result shown in Fig. 23 and it is illustrated that for a purely sine wave that has a constant shifted frequency, its time synchrophasor is also a constant angle. The range of time synchrophasors is $0 \sim \pi$, so time synchrophasors are symmetrical about the time axis its value is zero correspondence to the nominal frequency f_0. For example, time synchrophasor of the 55Hz frequency will agree with time synchrophasor of Fig.23 though their phasors are different.

Figure 24 shows the measured phasors and space synchrophasor simulation with parameters of Table IV. It is illustrated that space synchrophasor keeps an initial value when both frequencies equal each. This also illustrated that space synchrophasor could be obtained directly from two phasors with coordinated universal time (GPS) and no demands an analog reference wave that has nominal frequency.

Figure 25 shows the measured phasors and space synchrophasor simulation with parameters of Table V. It is illustrated that space synchrophasor changes when two frequencies are different. We can calculate the estimated time to the point of two nodes have same rotation phase angle as follows

$$t_{asy} = \frac{\varphi_{10} - \varphi_{20}}{2\pi(f_1 - f_2)} = \frac{80}{360 \times (51-49)} = 0.1111(s) \tag{38}$$

Figure 26 shows the measured phasors and space synchrophasor simulation with parameters of Table VI. It is illustrated that space synchrophasor changes between $0 \sim \pi$ and always possesses a positive value, though it has increasing mode and decreasing mode. The elapsed time of a phase angle π can be calculated as follows

$$t_{\pi} = \frac{\pi}{2\pi(f_1 - f_2)} = \frac{1}{2(53-50)} = 0.1667(s) \tag{39}$$

TABLE IV
PARAMETERS USED FOR CASE4 SIMULATION

Input Frequency		Initial angle		Amplitude
Node1	Node2	Node1	Node2	
50HZ	50HZ	0DEG	-80DEG	45V

TABLE V
PARAMETERS USED FOR CASE5 SIMULATION

Input Frequency		Initial angle		Amplitude
Node1	Node2	Node1	Node2	
51HZ	49HZ	0DEG	80DEG	45V

TABLE VI
PARAMETERS USED FOR CASE6 SIMULATION

Input Frequency		Initial angle		Amplitude
Node1	Node2	Node2	Node2	
53HZ	50HZ	0DEG	80DEG	45V

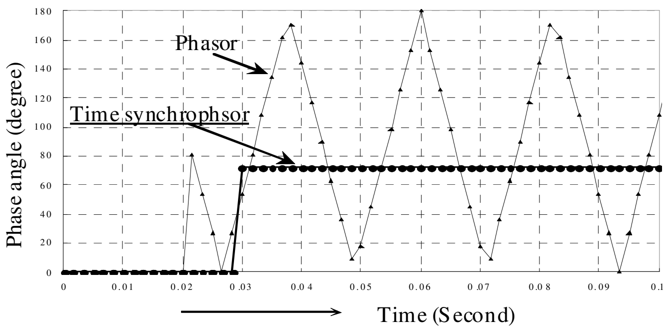

Fig. 23. Measured phasor and time synchrophasor with the proposed method (Case2).

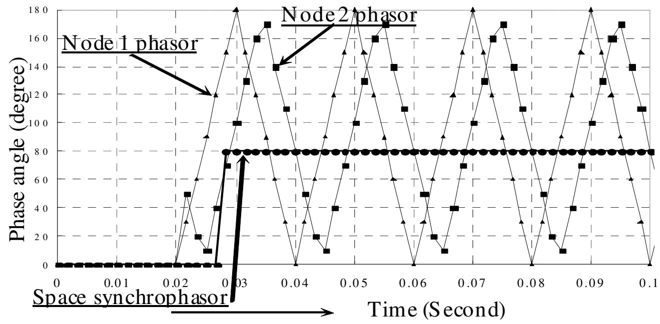

Fig. 24. Measured phasors and space synchrophasor with the proposed method (Case4).

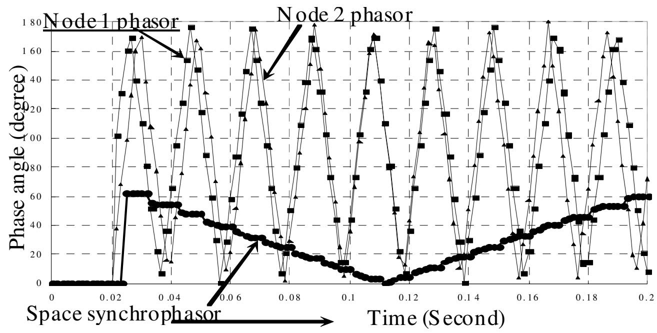

Fig.25. Measured phasors and space synchrophasor with the proposed method (Case5).

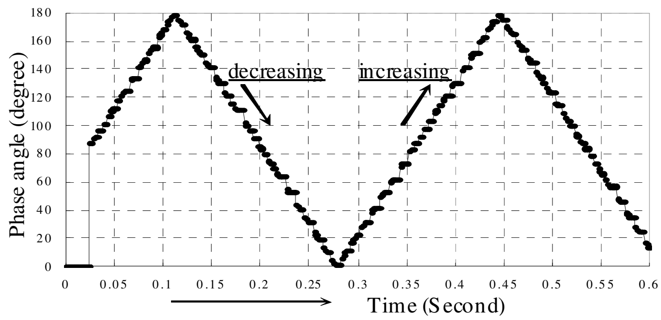

Fig. 26. Measured space synchrophasor with the proposed method (Case6).

V. Analysis of Accuracy, Step Test and Harmonic Distortions Influence of the Proposed Method

This section analyzes accuracy, step test and harmonic distortion influence of the proposed method with IEEE Standard C27.118-2005 [4] instead of comparing to conventional methods.

A. Accuracy and the TVE index

According to [4], the TVE (total vector error) index is defined as follows.

$$TVE = \sqrt{\frac{(X_r(n) - X_r)^2 + (X_i(n) - X_i)^2}{X_r{}^2 + X_i{}^2}} \quad (40)$$

where $X_r(n)$ and $X_i(n)$ are the measured values, given by the measuring device, and X_r and X_i are the theoretical values of the input signal at the instant of time of measurement, determined from following (41) and the known conditions of X_m, ω, and φ.

$$X = X_r + jX_i = \frac{X_m}{\sqrt{2}} e^{j\varphi} \quad (41)$$

According to the proposed method, it is understood that the following equation is realized. (Refer to (22)-(28)).

$$\left.\begin{aligned} X_r(n) &= X_r = v_{est}(t) \\ X_i(n) &= X_i = v_{est}(t - \frac{1}{4f_1}) \end{aligned}\right\} \quad (42)$$

where $v_{est}(t)$ is the estimated data with the least square method using the measured frequency f_1 and $v_{est}(t-1/(4f_1))$ is the imaginary part of the voltage vector. Substituting (42) into (40), we obtain the error index as follows.

$$TVE = 0 \quad (43)$$

Because of the above (43), we suggest that using time synchrophasor as the error index for synchrophasors.

B. Magnitude step test

According to [4], a magnitude step test (10%) defined as follows.

$$\left.\begin{aligned} v(t < t_0) &= V_{m1}\cos(\omega t + \varphi) \\ v(t = t_0) &= \frac{V_{m1} + V_{m2}}{2}\cos(\omega t + \varphi) \\ v(t > t_0) &= V_{m2}\cos(\omega t + \varphi) \end{aligned}\right\} \quad (43)$$

The magnitude step test with parameters of Table VII and the simulation results are illustrated in Fig. 27-28. Figure 27 shows that the measured amplitude and chord length could follow the changing of the objective system quickly. Figure 28 shows that the transient influence is small and disappear fast in magnitude step test.

C. Phase step test

According to [4], a phase step test (90°) defined as follows.

$$\left.\begin{aligned} v(t < t_0) &= V_m\cos(\omega t + \varphi) \\ v(t = t_0) &= V_m\cos(\omega t + \varphi + \frac{\pi}{4}) \\ v(t > t_0) &= V_m\cos(\omega t + \frac{\pi}{2}) \end{aligned}\right\} \quad (44)$$

TABLE VII
PARAMETERS USED FOR MAGNITUDE STEP TEST (10%)

Input Frequency	t_0	V_{m1}	V_{m2}
50Hz	0.06s	1.414V	1.273 V

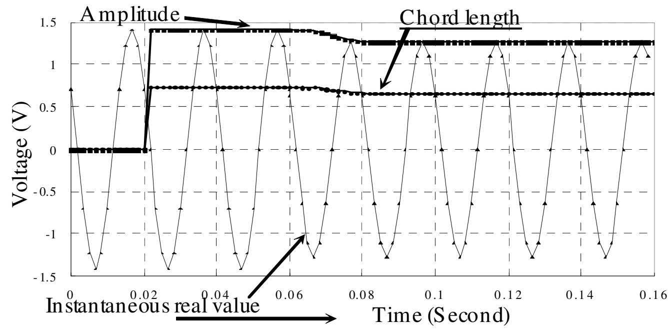

Fig. 27. Voltage instantaneous real values, measured amplitude and chord length in the magnitude step test (10%).

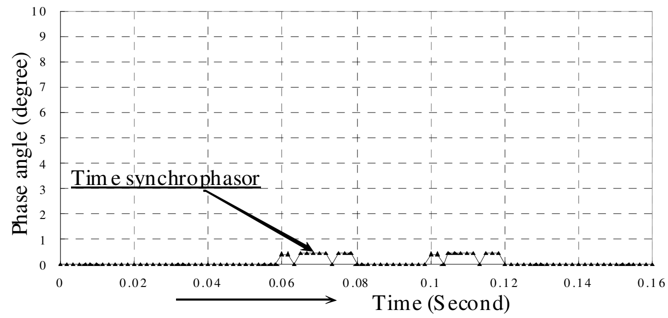

Fig. 28. Time synchrophasor in the magnitude step test (10%).

TABLE VIII
PARAMETERS USED FOR PHASE STEP TEST (90°)

Input Frequency	t_0	$d\varphi$	V_m(V)
50Hz	0.06s	90°	1.414V

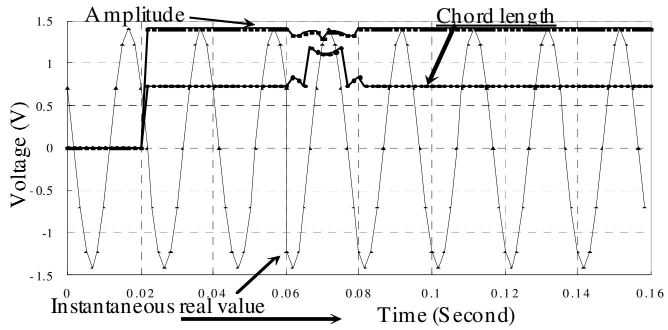

Fig. 29. Voltage instantaneous real values, measured amplitude and chord length in the phase step test (90°).

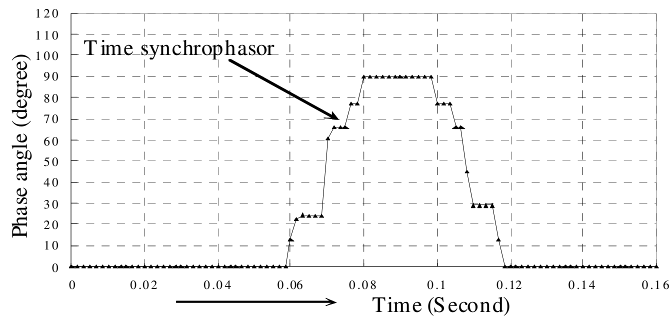

Fig. 30. Time synchrophasor in the phase step test (90°).

The phase step test with parameters of Table VIII and the simulation results are illustrated in Fig. 29-30. Figure 29 shows that the voltage flicker (phase shifting) influence only short time. Figure 30 shows that in the transient state, one 90° step is detected by the time synchrophasor and it disappears fast in phase step test.

D. Frequency step test

According to (4), a frequency step test (+5Hz) defined as follows.

$$\left.\begin{array}{l} v(t<t_0)=V_m\cos(2\pi f\,t+\varphi) \\ v(t=t_0)=V_m \\ v(t>t_0)=V_m\cos[2\pi(f+5)t+\varphi] \end{array}\right\} \tag{45}$$

The magnitude step test with parameters of Table IX and the simulation results are illustrated in Fig. 31-33. Similar with figure 31, figure 33 shows that the measured frequency could follow the changing of the objective system quickly. Figure 32 shows that the time synchrophasor has a constant value even in a shifted frequency (55Hz).

From above results, it could find that the range of synchrophasors are *0 ~ π* with the proposed method that is different from conventional methods theirs range are *-π~ π*.

TABLE IX
PARAMETERS USED FOR FREQUENCY STEP TEST (+5HZ)

Input Frequency	t_0	df	V_m(V)
50Hz	0.06s	5Hz	1.414V

E. Reduction of harmonic distortions influence

Because harmonic distortions affect the precision of the frequency and the synchrophasors measurement, we introduce moving average processes to reduce its influence. The average amplitude could be obtained by using result of (13) as follows.

$$V_{ave}(t)=\frac{1}{N}\sum_{n=0}^{N-1}V(t-nT) \tag{46}$$

where *N* is an integer number of sampling points. The average chord length could be obtained by using result of (15) as follows.

$$V_{2ave}(t)=\frac{1}{N}\sum_{n=0}^{N-1}V_2(t-nT) \tag{47}$$

In (18), we use average amplitude and chord length instead of instantaneous values respectively.

At last, the average frequency could be obtained by using result of (20) as follows.

$$f_{1ave}(t)=\frac{1}{N}\sum_{n=0}^{N-1}f_1(t-nT) \tag{48}$$

A harmonic distortions simulation with parameters of Table X is executed and the result is illustrated in Fig. 34. The length of moving average time is set to two period times. Figure 34 shows the error of measured frequency is less than 0.5% even in a state there are big harmonic distortions (Random 10%V1).

TABLE X
PARAMETERS USED FOR CASE7 SIMULATION

Input Frequency	Amplitude, V1	Distortion
50HZ	45V	Random, ±10%V1

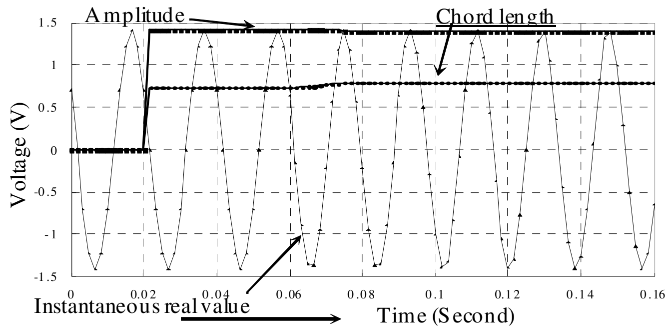

Fig. 31. Voltage instantaneous real values, measured amplitude and chord length in the frequency step test (+5Hz).

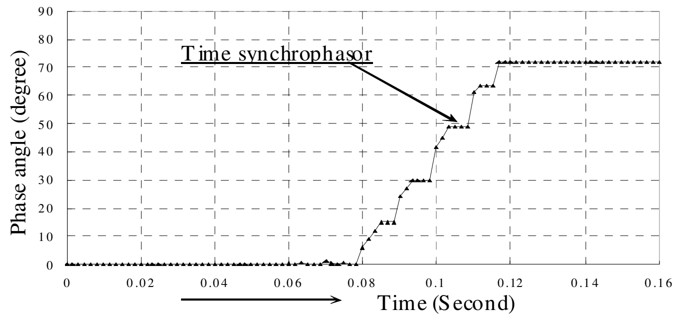

Fig. 32. Time synchrophasor in the frequency step test (+5Hz).

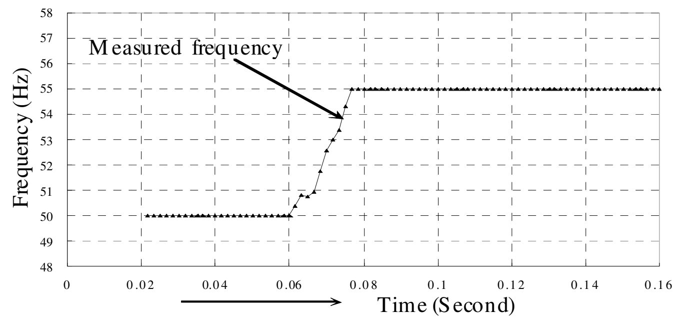

Fig. 33. Measured frequency in the frequency step test (+5Hz).

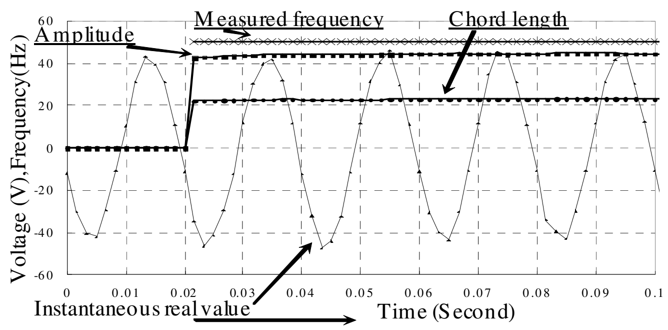

Fig. 34. Voltage instantaneous real values, measured amplitude and chord length in Case 7. (A harmonic distortions example)

VI. CONCLUSIONS

The paper considered that for measuring synchrophasors, the actual frequency should be measured first. After introduced a novel frequency measuring method with difference integral equations its solution agrees with Nyquist–Shannon sampling theorem, the phasor is defined in the upper half-plane and measured with least square method. Then, space synchrophasor is defined as phasor difference between a space interval (two nodes). Furthermore, time synchrophasors is defined as phasor difference between of a time interval (one or several period times). These two type synchrophasors are measured with the proposed method and sometimes synchrophasors can't be determined uniquely so we introduced the uncertainty principles into measurement. The proposed method can deal with issues arising from actual frequency that shifts the nominal frequency. The phasor, time synchrophasor and space synchrophasor are changing from $0 \sim \pi$ in the upper half plane that always have positive values. The paper illustrated that the proposed method is practical with numerical simulation examples. At last, the paper analyzed accuracy, step test and harmonic distortions influence of the proposed method. The paper proposed a digital thinking synchrophasors measuring method and it could be improved more and more. It is believed that the proposed method will replace these methods that based upon analog thinking in future.

VII. REFERENCES

Periodicals:

[1] A.G. Phadke, J.S. Thorp, M.G. Adamiak, "A New Measurement Technique for Tracking Voltage Phasors, Local System Frequency, and Rate of Change of Frequency," *IEEE Transactions on Power Apparatus and Systems*, vol. PAS-102, no. 5, pp1025-1038, May 1983.

Books:

[2] S. Yamamura, *Spiral Vector Theory of AC Circuits and Machines*, Oxford University Press, 1992, pp. 3-9.

Papers from Conference Proceedings (Published):

[3] K. Seki, "Development of Active Filters with Spiral Vector Theory," in *Power Conversion Conference – Nagoya, 2007, pp526-533*

Standards:

[4] *IEEE Synchrophasor Standard*, IEEE Standard C37.118-2005.

Patents:

[5] K. Seki, "Frequency measuring device," U.S. Patent 6 985 824, Feb. 23, 2004.

[6] K. Seki, "Synchronous vector measuring device," U.S. Patent 7 006 935, Jun. 23, 2004.